



Research article

Rich dynamics of a three-tiered anaerobic food-web in a chemostat with multiple substrate inflow

Szymon Sobieszek¹, Matthew J. Wade^{2,*} and Gail S. K. Wolkowicz¹

¹ Department of Mathematics and Statistics, McMaster University, Hamilton, ON L8S 4K1, Canada

² School of Engineering, Newcastle University, Newcastle-upon-Tyne NE1 7RU, United Kingdom

* **Correspondence:** Email: matthew.wade@newcastle.ac.uk.

Abstract: The mathematical analysis of a three-tiered food-web describing anaerobic chlorophenol mineralisation has suggested the emergence of interesting dynamical behaviour through its specific ecological interactions, which include competition, syntrophy, and product inhibition. Previous numerical analyses have revealed the possibility of a Hopf bifurcation at the interior equilibrium as well as the role of extraneous substrate inputs in both mitigating the emergence of periodic solutions and expanding the desired operating region where the positive steady-state is stable and full mineralisation occurs. Here we show that, for a generalised model, the inflow of multiple substrates results in greater dynamical complexity and show the occurrence of a supercritical Hopf bifurcation resulting from variations in these operating parameters. Further, using numerical estimation, we also show that variations in the dilution rate can lead to Bogdanov-Takens and Bautin bifurcations. Finally, we are able to apply persistence theory for a range of parameter sets to demonstrate persistence in cases where chlorophenol and hydrogen are extraneously added to the system, mirroring recent applied studies highlighting the role of hydrogen in maintaining stable anaerobic microbial communities.

Keywords: chlorophenol mineralisation; mathematical modelling; bifurcation analysis; Hopf bifurcation; hydrogen

1. Introduction

A mathematical model of the complete anaerobic mineralisation of a generic monochlorophenol isomer (C_6H_4ClOH) by a canonical food-web has recently been described [1]. The system comprises three microbial species (chlorophenol degrader, phenol degrader, hydrogenotrophic methanogen). Their interactions are summarised as follows:

- Reductive dehalogenation of chlorophenol in the presence of hydrogen by the chlorophenol degrader producing phenol [2];

- Phenol is mineralised by a phenol degrader to acetate and hydrogen via the benzoyl-CoA pathway or a caproate intermediary [3];
- Anaerobic acetogenic (acetate producing) processes are known to be endergonic (the reaction results in a net loss of energy to the system). The production of hydrogen can lead to thermodynamic constraints, or inhibition, if its partial pressure is high enough. In other words, the reaction becomes decreasingly exergonic as more hydrogen is produced until it ceases to be thermodynamically favourable [4, 5]. Hydrogen scavengers such as the hydrogenotrophic methanogen form a syntrophic partnership with the phenol degrader by maintaining the hydrogen partial pressure at concentrations low enough for the mineralisation reaction to proceed;
- Given that the chlorophenol degrader may also act as a syntrophic partner with the phenol degrader, a competitive interaction between the two hydrogen utilisers occurs. These positive and negative feedback loops reframe the ecological network from a simple food-chain to a more complex food-web that allows for the possibility of periodicity. This additionally allows for the case where the system reduces to a self-sustaining two-species network in which the chlorophenol degrader acts as the syntrophic partner to the phenol degrader.

A diagrammatic representation of the food-web is presented in Figure 1. The model is a simplified representation of the system at the population level, ignoring metabolic intermediates and ‘dead-end’ products such as methane, which do not contribute to the process dynamics. Acetoclastic methanogenesis, the conversion of acetate to methane, is also omitted from the model.

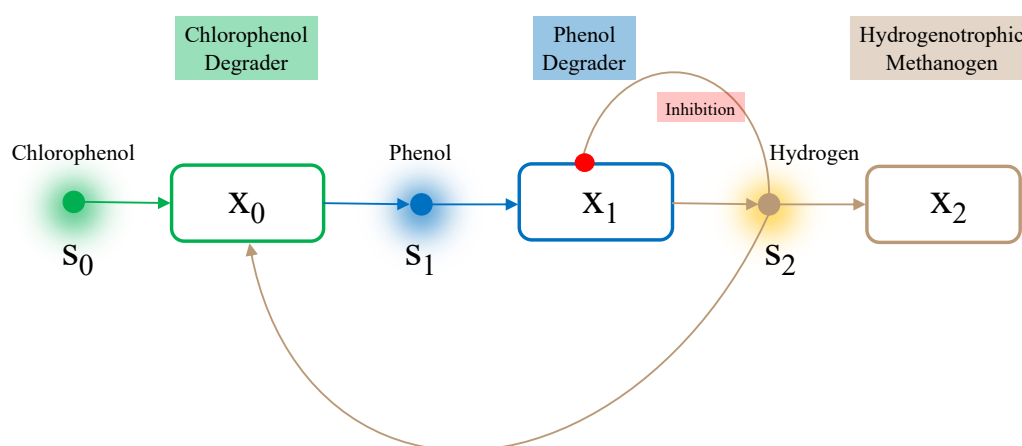


Figure 1. Schematic of the three-tiered food-web described by the model under analysis here. The state variables $[x_i, s_i, i = 0, 1, 2]$ used in the model are also indicated.

Hydrogen, however, has been shown to play an important role in stability of anaerobic microbial communities through the effects of inhibition and competition [6–8]. Given that external hydrogen addition will maintain the methanogen population (no washout when the methanogen growth rate is greater than the combined dilution and decay/maintenance rates) under a wider operating parameter regime (chlorophenol inflow and dilution rate) [1], a global analysis of the model can provide deeper insights into the ecological role of hydrogen through its association with community stability and criticality of the Hopf bifurcation.

Here, we focus on the mathematical analysis of the model, extending the work reported in the literature. For example, an analytical approach was taken to characterise the existence and stability of the system equilibria with and without inclusion of a microbial decay constant using a general representation of the species growth functions [9]. With no decay and without considering production of hydrogen by the phenol degrader, (an unusual constraint that appears to make the system entirely theoretical with extraneous addition of hydrogen necessary for complete chlorophenol mineralisation) local stability and the conditions giving rise to asymptotic coexistence of all three species have been shown analytically, with the possibility of periodic orbits not excluded [10]. Numerical analysis has suggested the presence of a Hopf bifurcation of the positive steady-state, with the concentration of influent chlorophenol as the bifurcating parameter [9].

In this work, we extend the analysis of the model to provide a proof of the existence and uniqueness of system equilibria and their stability for the most general case where up to three external inputs (chlorophenol, phenol, hydrogen) may be included. The procedure we use allows us to identify sufficient conditions for the emergence of a Hopf bifurcation as the inflow concentration parameters vary. We are also able to prove that there is a range of parameters for which the model is uniformly persistent, i.e., all populations avoid extinction, a new result for the system. Two-parameter bifurcation diagrams reveal rich dynamics that include Bogdanov-Takens and Bautin bifurcations and, hence, homoclinic and saddle-node of limit cycle bifurcations.

2. The model revisited

We first present concisely the original given by [1] using the identical scaling:

$$\begin{cases} x'_0 &= -\alpha x_0 + \mu_0(s_0, s_2) x_0 - k_A x_0, \\ x'_1 &= -\alpha x_1 + \mu_1(s_1, s_2) x_1 - k_B x_1, \\ x'_2 &= -\alpha x_2 + \mu_2(s_2) x_2 - k_C x_2, \\ s'_0 &= \alpha(u_f - s_0) - \mu_0(s_0, s_2) x_0, \\ s'_1 &= \alpha(u_g - s_1) + \omega_0 \mu_0(s_0, s_2) x_0 - \mu_1(s_1, s_2) x_1, \\ s'_2 &= \alpha(u_h - s_2) - \omega_2 \mu_0(s_0, s_2) x_0 + \omega_1 \mu_1(s_1, s_2) x_1 - \mu_2(s_2) x_2, \end{cases} \quad (2.1)$$

with

$$\begin{aligned} \alpha &= \frac{D}{k_{m, \text{ch}} Y_{\text{ch}}}, \\ u_f &= \frac{S_{\text{ch}, \text{in}}}{K_{S, \text{ch}}}, \quad u_g = \frac{S_{\text{ph}, \text{in}}}{K_{S, \text{ph}}}, \quad u_h = \frac{S_{\text{H}_2, \text{in}}}{K_{S, \text{H}_2}}, \\ \omega_0 &= \frac{K_{S, \text{ch}}}{K_{S, \text{ph}}} \frac{224}{208} (1 - Y_{\text{ch}}), \quad \omega_1 = \frac{K_{S, \text{ph}}}{K_{S, \text{H}_2}} \frac{32}{224} (1 - Y_{\text{ph}}), \quad \omega_2 = \frac{16}{208} \frac{K_{S, \text{ch}}}{K_{S, \text{H}_2}}, \\ \phi_1 &= \frac{k_{m, \text{ph}} Y_{\text{ph}}}{k_{m, \text{ch}} Y_{\text{ch}}}, \quad \phi_2 = \frac{k_{m, \text{H}_2} Y_{\text{H}_2}}{k_{m, \text{ch}} Y_{\text{ch}}}, \\ K_P &= \frac{K_{S, \text{H}_2, \text{c}}}{K_{S, \text{H}_2}}, \quad K_I = \frac{K_{S, \text{H}_2}}{K_{I, \text{H}_2}}, \end{aligned}$$

$$k_A = \frac{k_{\text{dec, ch}}}{k_{\text{m, ch}} Y_{\text{ch}}}, \quad k_B = \frac{k_{\text{dec, ph}}}{k_{\text{m, ch}} Y_{\text{ch}}}, \quad k_C = \frac{k_{\text{dec, H}_2}}{k_{\text{m, ch}} Y_{\text{ch}}}.$$

$$\mu_0(s_0, s_2) = \frac{s_0}{1 + s_0} \frac{s_2}{K_P + s_2}, \quad \mu_1(s_1, s_2) = \frac{\phi_1 s_1}{1 + s_1} \frac{1}{1 + K_I s_2}, \quad \mu_2(s_2) = \frac{\phi_2 s_2}{1 + s_2}, \quad (2.2)$$

where α is the dilution rate, u_f, u_g, u_h are the chlorophenol, phenol, and hydrogen inflow concentrations, respectively, and k_A, k_B, k_C are the decay (or maintenance) terms. These are scaled to be dimensionless, as are the other parameters using the scaling provided by [1]. Briefly, $k_{\text{m}, \cdot}$ are the specific growth rates, $K_{\text{S}, \cdot}$ are the half-saturation coefficients, Y_{\cdot} are the substrate yield coefficients, $K_{\text{I, H}_2}$ is the kinetic inhibition constant of hydrogen on the phenol degrader, and $k_{\text{dec}, \cdot}$ are the unscaled decay terms. The numeric values indicate the stoichiometric coefficients given in terms of units of Chemical Oxygen Demand rather than molarity, as is common for environmental engineering models. The $\mu_n(\cdot), n = 0, 1, 2$ are the species growth functions described by double Monod, Monod with product inhibition, and Monod kinetics, respectively. Subscripts $\cdot_{\text{ch}}, \cdot_{\text{ph}}, \cdot_{\text{H}_2}$ relate to the chlorophenol degrader, phenol degrader, and methanogen, respectively.

For the numerical bifurcation analysis given in Section 4.4, we consider the same parameter values as provided in the original work in [1], as shown in Table 1.

Table 1. Parameter values for system (2.1).

Parameters	Value
ω_0	0.1854
ω_1	1656.69
ω_2	163.08
ϕ_1	1.8875
ϕ_2	3.8113
K_P	0.04
K_I	7.1429

3. Reduction of the model

We are able to obtain many theoretical results assuming general forms of the growth functions provided we assume the death rates of the microbial populations are insignificant compared to the dilution rate. We thus consider the following system that is identical to system (2.1), except that we assume $k_i = 0$,

$i \in \{A, B, C\}$:

$$\begin{cases} x_0' &= -\alpha x_0 + \mu_0(s_0, s_2) x_0, \\ x_1' &= -\alpha x_1 + \mu_1(s_1, s_2) x_1, \\ x_2' &= -\alpha x_2 + \mu_2(s_2) x_2, \\ s_0' &= \alpha(u_f - s_0) - \mu_0(s_0, s_2) x_0, \\ s_1' &= \alpha(u_g - s_1) + \omega_0 \mu_0(s_0, s_2) x_0 - \mu_1(s_1, s_2) x_1, \\ s_2' &= \alpha(u_h - s_2) - \omega_2 \mu_0(s_0, s_2) x_0 + \omega_1 \mu_1(s_1, s_2) x_1 - \mu_2(s_2) x_2, \end{cases} \quad (3.1)$$

$$x_i(0) \geq 0, \quad s_i(0) \geq 0, \quad i \in \{0, 1, 2\}.$$

We assume that $\mu_0(s_0, s_2)$, $\mu_1(s_1, s_2)$, $\mu_2(s_2)$ are C^1 functions that satisfy the following general conditions:

- (H1) For all $s_0 \geq 0$ and $s_2 \geq 0$, $\mu_0(0, s_2) = 0$, $\mu_0(s_0, 0) = 0$. As a consequence, $\partial_{s_0} \mu_0(s_0, 0) = 0$, $\partial_{s_2} \mu_0(0, s_2) = 0$. Thus we assume that the chlorophenol degrader cannot grow in the absence of either chlorophenol or hydrogen;
- (H2) For all $s_0 > 0$ and $s_2 > 0$, $\partial_{s_0} \mu_0(s_0, s_2) > 0$, $\partial_{s_2} \mu_0(s_0, s_2) > 0$. Thus we assume that the chlorophenol degrader grows on both chlorophenol and hydrogen;
- (H3) For all $s_2 \geq 0$, $\mu_1(0, s_2) = 0$. As a consequence $\partial_{s_2} \mu_1(0, s_2) = 0$. Thus we assume that the phenol degrader cannot grow in the absence of phenol;
- (H4) For all $s_1 > 0$ and $s_2 > 0$, $\partial_{s_1} \mu_1(s_1, s_2) > 0$, $\partial_{s_2} \mu_1(s_1, s_2) < 0$. Thus we assume that the supply of phenol results in growth of the phenol degrader, and that hydrogen inhibits its growth;
- (H5) $\mu_2(0) = 0$ and $\mu_2'(s_2) > 0$ for all $s_2 > 0$. Thus we assume that the methanogen cannot grow without the presence of hydrogen, and that increasing the supply of hydrogen results in faster growth of the methanogen.

We use the prototypes μ_0 , μ_1 , and μ_2 defined in Eq (2.2), which satisfy these conditions, when we are unable to prove results in general, and when providing numerical simulations or bifurcation diagrams.

The proof of the following lemma, needed for well-posedness of system (3.7), is standard, and hence omitted.

Lemma 3.1. *All solutions of system (3.1) with positive initial conditions remain positive and bounded for all positive times and if $x_i(0) = 0$, $i \in \{0, 1, 2\}$, then $x_i(t) = 0$ for all $t \geq 0$.*

We can further simplify analysis of system (3.1) using the following lemma.

Lemma 3.2. *The omega limit set of any solution of system (3.1) is contained in a positively invariant attracting set $\Omega \subset \mathbb{R}^6$ defined as*

$$\begin{aligned} \Omega = \{ & (x_0, x_1, x_2, s_0, s_1, s_2) \in \mathbb{R}^6 : x_i, s_i \geq 0, i = 0, 1, 2; \\ & x_0 + s_0 = u_f, \\ & x_1 + \omega_0 s_0 + s_1 = \omega_0 u_f + u_g, \\ & \omega_2 x_0 + x_2 + \omega_0 \omega_1 s_0 + \omega_1 s_1 + s_2 = \omega_0 \omega_1 u_f + \omega_1 u_g + u_h \}. \end{aligned} \quad (3.2)$$

Proof. By adding the first and the fourth equations of system (3.1), we obtain

$$x'_0 + s'_0 = -\alpha(x_0 + s_0 - u_f),$$

hence

$$(x_0 + s_0 - u_f)' = -\alpha(x_0 + s_0 - u_f),$$

which implies that

$$x_0(t) + s_0(t) = u_f + (x_0(0) + s_0(0) - u_f)e^{-\alpha t}. \quad (3.3)$$

Similarly, we obtain

$$x_1(t) + \omega_0 s_0(t) + s_1(t) = \omega_0 u_f + u_g + (x_1(0) + \omega_0 s_0(0) + s_1(0) - \omega_0 u_f - u_g)e^{-\alpha t}, \quad (3.4)$$

and

$$\begin{aligned} \omega_2 x_0(t) + x_2(t) + \omega_0 \omega_1 s_0(t) + \omega_1 s_1(t) + s_2(t) &= \omega_0 \omega_1 u_f + \omega_1 u_g + u_h + \\ &+ (\omega_0 x_0(0) + x_2(0) + \omega_0 \omega_1 s_0(0) + \omega_1 s_1(0) + s_2(0) - \omega_0 \omega_1 u_f - \omega_1 u_g - u_h)e^{-\alpha t}. \end{aligned} \quad (3.5)$$

By taking the limit as $t \rightarrow \infty$ in Eqs (3.3)–(3.5) we obtain

$$\begin{aligned} \lim_{t \rightarrow \infty} (x_0(t) + s_0(t)) &= u_f, \\ \lim_{t \rightarrow \infty} (x_1(t) + \omega_0 s_0(t) + s_1(t)) &= \omega_0 u_f + u_g, \\ \lim_{t \rightarrow \infty} (\omega_2 x_0(t) + x_2(t) + \omega_0 \omega_1 s_0(t) + \omega_1 s_1(t) + s_2(t)) &= \omega_0 \omega_1 u_f + \omega_1 u_g + u_h, \end{aligned}$$

which yields the desired result. \square

The three equalities in the definition of Ω given in system (3.2) are called “conservation principles”. Using them, we can compute s_0 , s_1 , and s_2 as functions of x_0 , x_1 , x_2 :

$$\begin{aligned} s_0 &= -x_0 + u_f, \\ s_1 &= \omega_0 x_0 - x_1 + u_g, \\ s_2 &= -\omega_2 x_0 + \omega_1 x_1 - x_2 + u_h. \end{aligned} \quad (3.6)$$

Now, we can reduce the analysis of the original system (3.1) to the analysis of the following three-dimensional limiting system on the invariant set Ω :

$$\begin{cases} x'_0 = -\alpha x_0 + \mu_0(-x_0 + u_f, -\omega_2 x_0 + \omega_1 x_1 - x_2 + u_h)x_0, \\ x'_1 = -\alpha x_1 + \mu_1(\omega_0 x_0 - x_1 + u_g, -\omega_2 x_0 + \omega_1 x_1 - x_2 + u_h)x_1, \\ x'_2 = -\alpha x_2 + \mu_2(-\omega_2 x_0 + \omega_1 x_1 - x_2 + u_h)x_2. \end{cases} \quad (3.7)$$

From now on, we will study the reduced system (3.7). We begin by analysing all the possible equilibria.

3.1. Equilibria of the reduced system and their local stability

The equilibria are found by setting the right hand sides of Eq (3.7) equal to zero. Below, we list all the possibilities obtained this way. Since Eq (3.6) give a one-to-one correspondence of the equilibria of system (3.7) with the equilibria of system (3.1), we also list the corresponding steady states $(x_0, x_1, x_2, s_0, s_1, s_2)$ of the six-dimensional system in each case. Each equilibrium is preceded by a subscript, indicating which population of microorganisms survives. That is, subscript (100) implies that $x_0 > 0, x_1 = x_2 = 0$, (110) that $x_0, x_1 > 0, x_2 = 0$, and so on.

Types of equilibria of system (3.7):

- Zero equilibrium $_{(000)}\mathcal{E} = (0, 0, 0)$. The corresponding equilibrium $_{(000)}\mathbb{E}$ in the six-dimensional system:

$$_{(000)}\mathbb{E} = (0, 0, 0, u_f, u_g, u_h).$$

In this case, all the populations die out, hence the only source for the substrates comes from the inflows u_f, u_g and u_h .

- Boundary equilibria:

– $_{(100)}\mathcal{E} = (_{(100)}x_0, 0, 0)$, where $x_0 = _{(100)}x_0 > 0$ is a solution (if it exists) of

$$\mu_0(-x_0 + u_f, -\omega_2 x_0 + u_h) = \alpha.$$

The corresponding equilibrium $_{(100)}\mathbb{E}$ in the six-dimensional system:

$$_{(100)}\mathbb{E} = (_{(100)}x_0, 0, 0, -_{(100)}x_0 + u_f, \omega_0 _{(100)}x_0 + u_g, -\omega_2 _{(100)}x_0 + u_h).$$

In this case, the only microorganism surviving is the chlorophenol degrader. It consumes the chlorophenol, hence the value of s_0 is given as the balance between this consumption, and the supply inflow u_f . Since x_0 produces phenol, this value is added to u_g to obtain the total phenol amount s_1 . Since x_0 consumes hydrogen as well, the value $\omega_2 _{(100)}x_0$ is subtracted from s_2 . This steady state is not desirable, because of the phenol build-up in the system.

– $_{(010)}\mathcal{E} = (0, _{(010)}x_1, 0)$, where $x_1 = _{(010)}x_1 > 0$ is a solution (if it exists) of

$$\mu_1(-x_1 + u_g, \omega_1 x_1 + u_h) = \alpha.$$

The corresponding equilibrium $_{(010)}\mathbb{E}$ in the six-dimensional system:

$$_{(010)}\mathbb{E} = (0, _{(010)}x_1, 0, u_f, -_{(010)}x_1 + u_g, \omega_1 _{(010)}x_1 + u_h).$$

In this case, only the phenol degrader survives, and hence the value of s_1 at the equilibrium is equal to the balance between its consumption and inflow u_g . Chlorophenol is not being consumed, hence its total amount equals the inflow concentration u_f . Hydrogen is being produced by the phenol degrader, and also its value is increased by the inflow u_h .

– $_{(001)}\mathcal{E} = (0, 0, _{(001)}x_2)$, where $x_2 = _{(001)}x_2 > 0$ is a solution (if it exists) of

$$\mu_2(-x_2 + u_h) = \alpha.$$

The corresponding equilibrium $_{(001)}\mathbb{E}$ in the six-dimensional system:

$$_{(001)}\mathbb{E} = (0, 0, _{(001)}x_2, u_f, u_g, -_{(001)}x_2 + u_h).$$

Here, only the methanogen is present, hence the values of chlorophenol and phenol are equal to the the inflow concentrations u_f and u_g , respectively.

$$-_{(101)}\mathcal{E} = (_{(101)}x_0, 0, -\omega_2 _{(101)}x_0 + u_h - \mu_2^{-1}(\alpha)),$$

where $x_0 = _{(101)}x_0 > 0$ is a solution (if it exists) of

$$\mu_0(-x_0 + u_f, \mu_2^{-1}(\alpha)) = \alpha.$$

The corresponding equilibrium $_{(101)}\mathbb{E}$ in the six-dimensional system:

$$_{(101)}\mathbb{E} = (_{(101)}x_0, 0, -\omega_2 _{(101)}x_0 + u_h - \mu_2^{-1}(\alpha), -_{(101)}x_0 + u_f, \omega_0 _{(101)}x_0 + u_g, \mu_2^{(-1)}(\alpha)).$$

In this case, both the chlorophenol degrader and the methanogen are present. The lack of the phenol degrader results in phenol build-up. We can also observe competition for hydrogen between the chlorophenol degrader and the methanogen.

$$-_{(011)}\mathcal{E} = (0, _{(011)}x_1, \omega_1 _{(011)}x_1 + u_h - \mu_2^{-1}(\alpha)),$$

where $x_1 = _{(011)}x_1 > 0$ is a solution (if it exists) of

$$\mu_1(-x_1 + u_g, \mu_2^{-1}(\alpha)) = \alpha.$$

The corresponding equilibrium $_{(011)}\mathbb{E}$ in the six-dimensional system:

$$_{(011)}\mathbb{E} = (0, _{(011)}x_1, \omega_1 _{(011)}x_1 + u_h - \mu_2^{-1}(\alpha), u_f, -_{(011)}x_1 + u_g, \mu_2^{-1}(\alpha)).$$

This steady state represents a two-tiered food chain, with the phenol degrader and methanogen present. Hydrogen has an inhibiting effect on the phenol degrader.

$$-_{(110)}\mathcal{E} = (_{(110)}x_0, _{(110)}x_1, 0), \text{ where } x_0 = _{(110)}x_0 > 0 \text{ and } x_1 = _{(110)}x_1 > 0 \text{ are solutions of}$$

$$\begin{aligned} \mu_0(-x_0 + u_f, -\omega_2 x_0 + \omega_1 x_1 + u_h) &= \alpha, \\ \mu_1(\omega_0 x_0 - x_1 + u_g, -\omega_2 x_0 + \omega_1 x_1 + u_h) &= \alpha. \end{aligned}$$

The corresponding equilibrium $_{(110)}\mathbb{E}$ in the six-dimensional system:

$$_{(110)}\mathbb{E} = (_{(110)}x_0, _{(110)}x_1, 0, -_{(110)}x_0 + u_f, \omega_0 _{(110)}x_0 - _{(110)}x_1 + u_g, -\omega_2 _{(110)}x_0 + \omega_1 _{(110)}x_1 + u_h).$$

In this case, both the chlorophenol and phenol degraders are present, however the methanogen is washed out. Thus, full mineralisation to methane is not possible. Hence, the hydrogen accumulates to some theoretical maximum, balanced such that the the inhibitory effect on the phenol degrader does not induce washout, whilst providing enough hydrogen for the chlorophenol degrader activity.

- Positive (interior) equilibrium ${}_{(111)}\mathcal{E} = (x_0^*, x_1^*, x_2^*)$, where $x_0 = x_0^* > 0$, $x_1 = x_1^* > 0$, and $x_2 = x_2^* > 0$ are solutions of

$$\begin{aligned}\mu_0(-x_0 + u_f, -\omega_2 x_0 + \omega_1 x_1 - x_2 + u_h) &= \alpha, \\ \mu_1(\omega_0 x_0 - x_1 + u_g, -\omega_2 x_0 + \omega_1 x_1 - x_2 + u_h) &= \alpha, \\ \mu_2(-\omega_2 x_0 + \omega_1 x_1 - x_2 + u_h) &= \alpha.\end{aligned}$$

The corresponding equilibrium ${}_{(111)}\mathbb{E}$ in the six-dimensional system:

$${}_{(111)}\mathbb{E} = (x_0^*, x_1^*, x_2^*, -x_0^* + u_f, \omega_0 x_0^* - x_1^* + u_g, \mu_2^{(-1)}(\alpha)).$$

Here, all species are present, and thus we observe full chlorophenol mineralisation. For this reason, asymptotic stability of this equilibrium is the desired operational state.

3.2. Existence, uniqueness, and local stability

The issues regarding the conditions on existence, uniqueness, and local stability of equilibria of the system have been fully answered in two recent preprints [11, 12]. The system considered in these works is more general, as it allows non-zero death rates. It is related to our system (3.1) by a linear change of variables, that is, by replacing x_0 by $\omega_0 \omega_1 x_0$, s_0 by $\omega_0 \omega_1 s_0$, x_1 by $\omega_1 s_1$, s_1 by $\omega_1 s_1$, and replacing ω_0 , ω_1 , and ω_2 by a single parameter $\omega = \frac{\omega_2}{\omega_0 \omega_1}$. It follows that all results described in [11, 12] apply to system (3.1) under this rescaling. Specifically, it has been shown that all equilibria, except ${}_{(110)}\mathbb{E}$, are unique, when they exist. Also, system (3.1) can have at most two equilibria of the form ${}_{(110)}\mathbb{E}$. Note that, following [1], different steady-state notation is adopted in [11, 12], i.e., ${}_{(000)}\mathbb{E} = \text{SS1}$, ${}_{(001)}\mathbb{E} = \text{SS2}$, ${}_{(100)}\mathbb{E} = \text{SS3}$, ${}_{(110)}\mathbb{E} = \text{SS4}$, ${}_{(101)}\mathbb{E} = \text{SS5}$, ${}_{(111)}\mathbb{E} = \text{SS6}$, ${}_{(010)}\mathbb{E} = \text{SS7}$, ${}_{(011)}\mathbb{E} = \text{SS8}$. For more details, we refer readers to the aforementioned preprints, as this paper is focused more on possible bifurcations and persistence analysis of system (3.7).

4. Analysis of the full system

4.1. Periodic orbits on the faces

We begin by ruling out the possibility of having a periodic orbit in one of the invariant faces of Ω . This can be done by using general forms of prototypes μ_0 , μ_1 and μ_2 .

Lemma 4.1. *There are no periodic orbits on the invariant faces of the set Ω of system (3.7).*

Proof. First, consider system (3.7) on the part of Ω with $x_0 = 0$, i.e..

$$\begin{cases} x_1' = (-\alpha + \mu_1(-x_1 + u_g, \omega_1 x_1 - x_2 + u_h)) x_1, \\ x_2' = (-\alpha + \mu_2(\omega_1 x_1 - x_2 + u_h)) x_2. \end{cases} \quad (4.1)$$

The domain for system (4.1) is given by the following set Ω_{12} :

$$\Omega_{12} = \{(x_1, x_2) \in \mathbb{R}^2 : 0 \leq x_1 \leq u_g, 0 \leq x_2 \leq u_h + \omega_1 x_1\}.$$

Notice that no periodic orbit can intersect the axes $x_1 = 0$ or $x_2 = 0$ since they are invariant. Now, let us define an auxiliary function

$$\varphi_0(x_1, x_2) = \frac{1}{x_1 x_2}, \quad (x_1, x_2) \in \Omega_{12} \setminus (\{x_1 = 0\} \cup \{x_2 = 0\}).$$

Then

$$\nabla \cdot (\varphi_0(-\alpha + \mu_1)x_1, \varphi_0(-\alpha + \mu_2)x_2) = \frac{-\partial_{s_1}\mu_1 + \omega_1\partial_{s_2}\mu_1}{x_2} - \frac{\mu'_2}{x_1} < 0$$

for all (x_1, x_2) in the domain of φ_0 , by Conditions (H4) and (H5). Thus, by the Dulac's Criterion [13], there are no periodic orbits in the $x_1 x_2$ face.

Now, consider system (3.7) on the part of Ω with $x_1 = 0$, i.e..

$$\begin{cases} x'_0 = (-\alpha + \mu_0(-x_0 + u_f, -\omega_2 x_0 - x_2 + u_h))x_0, \\ x'_2 = (-\alpha + \mu_2(-\omega_2 x_0 - x_2 + u_h))x_2, \end{cases}$$

defined on Ω_{02} given by

$$\Omega_{02} = \left\{ (x_0, x_2) \in \mathbb{R}^2 : 0 \leq x_0 \leq \min \left\{ u_f, \frac{u_h - x_2}{\omega_2} \right\}, 0 \leq x_2 \leq -\omega_2 x_0 + u_h \right\}.$$

For auxiliary function

$$\varphi_1(x_0, x_2) = \frac{1}{x_0 x_2}, \quad (x_0, x_2) \in \Omega_{02} \setminus (\{x_0 = 0\} \cup \{x_2 = 0\})$$

we have, using Conditions (H2) and (H5),

$$\nabla \cdot (\varphi_1(-\alpha + \mu_1)x_0, \varphi_1(-\alpha + \mu_2)x_2) = \frac{-\partial_{s_0}\mu_0 - \omega_2\partial_{s_2}\mu_0}{x_2} - \frac{\mu'_2}{x_0} < 0.$$

This, together with the fact that the axes $x_0 = 0$, $x_2 = 0$ are invariant, shows that there are no periodic orbits in the $x_0 x_2$ face.

Finally, consider system (3.7) on the part of Ω with $x_2 = 0$, i.e..

$$\begin{cases} x'_0 = (-\alpha + \mu_0(-x_0 + u_f, -\omega_2 x_0 + \omega_1 x_1 + u_h))x_0, \\ x'_1 = (-\alpha + \mu_1(\omega_0 x_0 - x_1 + u_g, -\omega_2 x_0 + \omega_1 x_1 + u_h))x_1. \end{cases}$$

defined on Ω_{01} given by

$$\Omega_{01} = \left\{ (x_0, x_1) \in \mathbb{R}^2 : 0 \leq x_0 \leq u_f, \max \left\{ 0, \frac{\omega_2 x_0 - u_h}{\omega_1} \right\} \leq x_1 \leq \omega_0 x_0 + u_g \right\}.$$

Analogously to the previous cases, we define

$$\varphi_2(x_0, x_1) = \frac{1}{x_0 x_1}, \quad (x_0, x_1) \in \Omega_{01} \setminus (\{x_0 = 0\} \cup \{x_1 = 0\})$$

and note that by Conditions (H2) and (H4)

$$\nabla \cdot (\varphi(-\alpha + \mu_0)x_0, \varphi(-\alpha + \mu_1)x_1) = \frac{-\partial_{s_0}\mu_0 - \omega_2\partial_{s_2}\mu_0}{x_1} + \frac{-\partial_{s_1}\mu_1 + \omega_1\partial_{s_2}\mu_1}{x_0} < 0.$$

Since the axes $x_0 = 0$, $x_1 = 0$ are invariant, by Dulac's Criterion, there are no periodic orbits in the x_0x_1 face. \square

4.2. Hopf bifurcation

In this work we are especially interested in developing a more systematic approach to studying the Hopf bifurcation of the interior equilibrium. That Hopf bifurcation that occurs in this model was previously observed numerically [9]. The occurrence of a stable periodic orbit in system (3.7) represents a situation in which the concentrations of all three populations of microorganisms oscillate indefinitely, and as a consequence, the substrate concentrations fluctuate.

The characteristic polynomial of the Jacobian corresponding to the interior equilibrium is given by

$$\lambda^3 + a_2\lambda^2 + a_1\lambda + a_0 = 0,$$

where

$$a_2 = -x_0^* \left(-\frac{\partial\mu_0}{\partial s_0} - \omega_2 \frac{\partial\mu_0}{\partial s_2} \right) - x_1^* \left(-\frac{\partial\mu_1}{\partial s_1} + \omega_1 \frac{\partial\mu_1}{\partial s_2} \right) + x_2^* \mu_2', \quad (4.2)$$

$$a_1 = x_1^* \frac{\partial\mu_1}{\partial s_1} \left(x_0^* \frac{\partial\mu_0}{\partial s_0} - (\omega_0\omega_1 - \omega_2) x_0^* \frac{\partial\mu_0}{\partial s_2} + x_2^* \mu_2' \right) + x_0^* \frac{\partial\mu_0}{\partial s_0} \left(-\omega_1 x_1^* \frac{\partial\mu_1}{\partial s_2} + x_2^* \mu_2' \right), \quad (4.3)$$

$$a_0 = x_0^* x_1^* x_2^* \frac{\partial\mu_0}{\partial s_0} \frac{\partial\mu_1}{\partial s_1} \mu_2', \quad (4.4)$$

and the coefficients a_2 , a_1 , and a_0 depend on the parameters u_f , u_g , u_h , and α . The coefficients a_2 and a_0 are sign-definite (they are both positive by Conditions (H2), (H4) and (H5)), but a_1 might possibly change sign. Notice first that since the polynomial is of order three, a real eigenvalue always exists. By the Routh-Hurwitz criterion, the above polynomial has a pair of purely imaginary eigenvalues if and only if

$$a_2a_1 = a_0 \quad (\text{which implies } a_1 > 0).$$

In that case, we also have

$$\lambda^3 + a_2\lambda^2 + a_1\lambda + a_0 = \lambda^3 + a_2\lambda^2 + a_1\lambda + a_2a_1 = (\lambda + a_2)(\lambda^2 + a_1).$$

Hence, the eigenvalues are $\lambda_1 = -a_2$ and $\lambda_{2,3} = \pm \sqrt{a_1}i$. In the following theorem, we prove that under certain nondegeneracy conditions, system (3.7) exhibits a Hopf bifurcation when the eigenvalues $\lambda_{1,2}$ cross the imaginary axis. We explore the possibility of a Hopf bifurcation in either of the three parameters u_f , u_g , or u_h . Additionally, the effect of α on possible bifurcations in the system is explored numerically, by constructing bifurcation diagrams in Subsection 4.4. To derive our results, we use specific forms of the growth functions (2.2) and the values of the parameters given in Table 1.

Theorem 4.1. Consider system (3.7) with the prototypes given by Eq (2.2) and with the values of parameters from Table 1 fixed. Define $f : \mathbb{R}_+^4 \rightarrow \mathbb{R}$ as $f(u_f, u_g, u_h, \alpha) = a_2 a_1 - a_0$ where a_0, a_1, a_2 are given in Eqs (4.2)–(4.4). Furthermore, assume that there exists a point $(u_f, u_g, u_h, \alpha) = (u_f^*, u_g^*, u_h^*, \alpha^*)$ such that $f(u_f^*, u_g^*, u_h^*, \alpha^*) = 0$. For fixed $u_g = u_g^*, u_h = u_h^*$, and $\alpha = \alpha^*$, denote the resulting third-order polynomial $f(u_f, u_g^*, u_h^*, \alpha^*)$ as

$$f(u_f, u_g^*, u_h^*, \alpha^*) = b_3 u_f^3 + b_2 u_f^2 + b_1 u_f + b_0,$$

for fixed $u_f = u_f^*, u_h = u_h^*$, and $\alpha = \alpha^*$, denote the resulting third-order polynomial $f(u_f^*, u_g, u_h^*, \alpha^*)$ as

$$f(u_f^*, u_g, u_h^*, \alpha^*) = c_3 u_g^3 + c_2 u_g^2 + c_1 u_g + c_0,$$

and for fixed $u_f = u_f^*, u_g = u_g^*$, and $\alpha = \alpha^*$, denote the second-order polynomial $f(u_f^*, u_g^*, u_h, \alpha^*)$ as

$$f(u_f^*, u_g^*, u_h, \alpha^*) = d_2 u_h^2 + d_1 u_h + d_0.$$

There exists a $\delta > 0$ such that, if $\|(u_f, u_g, u_h, \alpha) - (u_f^*, u_g^*, u_h^*, \alpha^*)\| < \delta$ and in addition:

I.

$$u_f^* \neq \frac{-b_2 \pm \sqrt{b_2^2 - 3b_1 b_3}}{3b_3},$$

then there is a Hopf bifurcation in u_f when $u_f = u_f^*$, or

II.

$$u_g^* \neq \frac{-c_2 \pm \sqrt{c_2^2 - 3c_1 c_3}}{3c_3},$$

then there is a Hopf bifurcation in u_g when $u_g = u_g^*$, or

III.

$$d_1^2 - 4d_2 d_0 \neq 0,$$

then there is a Hopf bifurcation in u_h when $u_h = u_h^*$.

Proof. Since eigenvalues are continuous functions of the parameters, we can see that if there is some $(u_f, u_g, u_h, \alpha) = (u_f^*, u_g^*, u_h^*, \alpha^*)$ such that $f(u_f^*, u_g^*, u_h^*, \alpha^*) = 0$ (i.e., $a_2 a_1 = a_0$), then if we denote by λ_1 the real eigenvalue (that always exists), there is some $\delta > 0$ such that for $\|(u_f, u_g, u_h, \alpha) - (u_f^*, u_g^*, u_h^*, \alpha^*)\| < \delta$, we always have $\lambda_1 < 0$. By Lemma 5.1, Section 5.2 in [13], this implies the existence of a parameter-dependent, smooth, attracting, two dimensional, center manifold $W_{(u_f, u_g, u_h, \alpha)}^c$. In the following analysis, we consider only parameters that are in the δ -neighbourhood of (u_f, u_g, u_h, α) , in order to ensure that the real eigenvalue λ_1 is negative.

By the Routh-Hurwitz criterion (since when ${}_{(111)}\mathcal{E}$ exists, a_0 and a_2 are always positive), a Hopf bifurcation occurs when the function f changes sign as a parameter varies. This ensures that the real part of a pair of complex eigenvalues with nonzero imaginary part passes through 0 and changes sign. This is related to the transversality condition: the derivative of the real part of the eigenvalue with

respect to the bifurcation parameter evaluated at the critical value when the real parts are zero is non-zero. We check this condition for specific forms of the functions μ_0 , μ_1 , and μ_2 , given in Eq (2.2). We begin our analysis by choosing u_f as the free parameter. We have

$$f(u_f, u_g^*, u_h^*, \alpha^*) = b_3 u_f^3 + b_2 u_f^2 + b_1 u_f + b_0,$$

for some constants b_i , $i \in \{0, 1, 2, 3\}$, and by the hypothesis, for $u_f = u_f^*$, we have $f(u_f^*, u_g^*, u_h^*, \alpha^*) = 0$. We want to find conditions on the coefficients of f that guarantee that its derivative with respect to u_f is not equal to zero when $u_f = u_f^*$. We have

$$\partial_{u_f} f(u_f, u_g^*, u_h^*, \alpha^*) = 3b_3 u_f^2 + 2b_2 u_f + b_1.$$

Thus $\partial_{u_f} f(u_f, u_g^*, u_h^*, \alpha^*) \neq 0$ if and only if

$$u_f^* \neq \frac{-b_2 \pm \sqrt{b_2^2 - 3b_1 b_3}}{3b_3}.$$

We have thus obtained a sufficient condition for a Hopf bifurcation.

If we choose u_g as the free parameter, we have

$$f(u_f^*, u_g, u_h^*, \alpha^*) = c_3 u_g^3 + c_2 u_g^2 + c_1 u_g + c_0,$$

for some constants c_i , $i \in \{0, 1, 2, 3\}$, and with the assumption that $f(u_f^*, u_g^*, u_h^*, \alpha^*) = 0$, by a similar analysis as in the previous case, we obtain an analogous sufficient condition for a Hopf bifurcation in u_g .

Finally, if we choose u_h as the free parameter, we have

$$f(u_f^*, u_g^*, u_h, \alpha^*) = d_2 u_h^2 + d_1 u_h + d_0, \quad (4.5)$$

for some constants d_i , $i \in \{0, 1, 2\}$. Once again, we assume that $f(u_f^*, u_g^*, u_h^*, \alpha^*) = 0$, that is

$$u_h^* = \frac{-d_1 \pm \sqrt{d_1^2 - 4d_2 d_0}}{2d_2}.$$

Here, $\partial_{u_h} f(u_f^*, u_g^*, u_h^*, \alpha^*) \neq 0$ if and only if $d_1^2 - 4d_2 d_0 \neq 0$.

□

We now illustrate the theoretical results with the numerical simulations. To approximate values of the equilibria, we used Maple software [14], rounding all the values to 6 significant digits. For the choice of parameters given in Table 1 and

$$\alpha = 0.01, \quad u_f = 0.5, \quad u_g = 0.0006,$$

it follows that the only zero of Eq (4.5) occurs for $u_h = 0.102520$. In Figure 2, we plot phase space for $u_h = 0.05$ (just before the Hopf bifurcation) using the ode15s solver from Matlab [15]. For this set of parameters, we have the following approximate values of the equilibria

$$\begin{aligned}
{}_{(000)}\mathcal{E} &= (0, 0, 0) \quad (\text{unstable}), \\
{}_{(100)}\mathcal{E} &= (0.000299015, 0, 0) \quad (\text{stable}), \\
{}_{(001)}\mathcal{E} &= (0, 0, 0.0473693) \quad (\text{unstable}), \\
{}_{(110)}\mathcal{E}^{(1)} &= (0.0545964, 0.00534486, 0) \quad (\text{unstable}), \\
{}_{(110)}\mathcal{E}^{(2)} &= (0.489465, 0.0487183, 0) \quad (\text{unstable}), \\
{}_{(111)}\mathcal{E} &= (0.306611, 0.0520205, 36.2277) \quad (\text{unstable}),
\end{aligned}$$

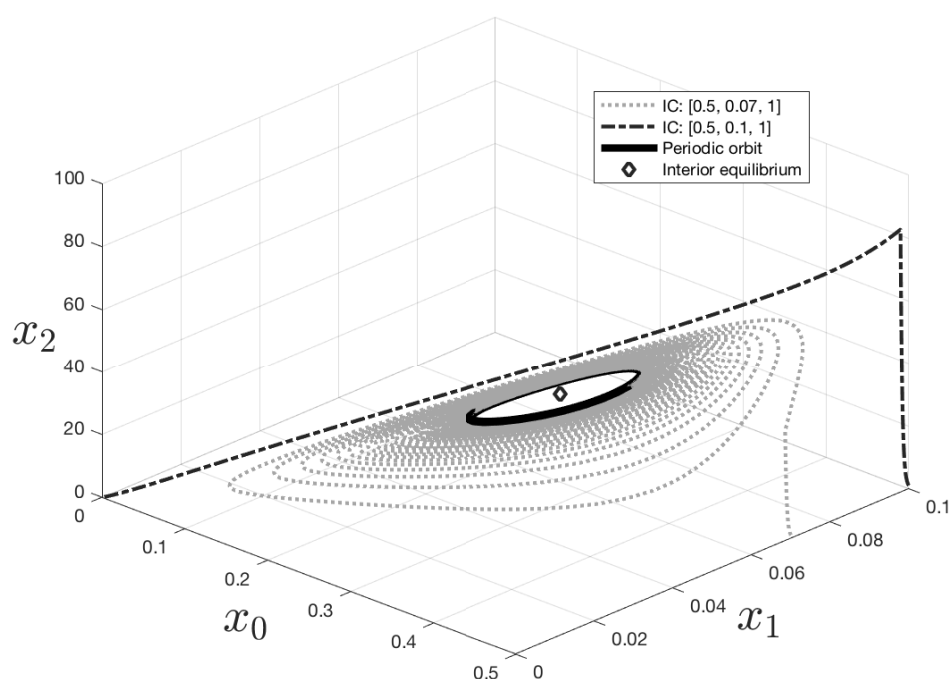


Figure 2. Phase space of system (3.7) with $\alpha = 0.01$, $u_f = 0.5$, $u_g = 0.0006$, and $u_h = 0.05$.

We can see that there exists a stable periodic orbit in the system, but depending on the initial conditions, the solution might also converge to the boundary equilibrium ${}_{(100)}\mathcal{E}$. Thus in this case we observe bistability.

We now repeat the simulations for $u_h = 0.3$ (after the predicted Hopf bifurcation), presented in Figure 3. With all the other parameters set to the same values as in the previous case, we have the following equilibria

$$\begin{aligned}
{}_{(000)}\mathcal{E} &= (0, 0, 0) \quad (\text{unstable}), \\
{}_{(100)}\mathcal{E} &= (0.00183202, 0, 0) \quad (\text{stable}), \\
{}_{(001)}\mathcal{E} &= (0, 0, 0.297369) \quad (\text{unstable}), \\
{}_{(110)}\mathcal{E}^{(1)} &= (0.0528596, 0.00502299, 0) \quad (\text{unstable}), \\
{}_{(110)}\mathcal{E}^{(2)} &= (0.489467, 0.0485697, 0) \quad (\text{unstable}), \\
{}_{(111)}\mathcal{E} &= (0.306611, 0.0520205, 36.4777) \quad (\text{stable}).
\end{aligned}$$

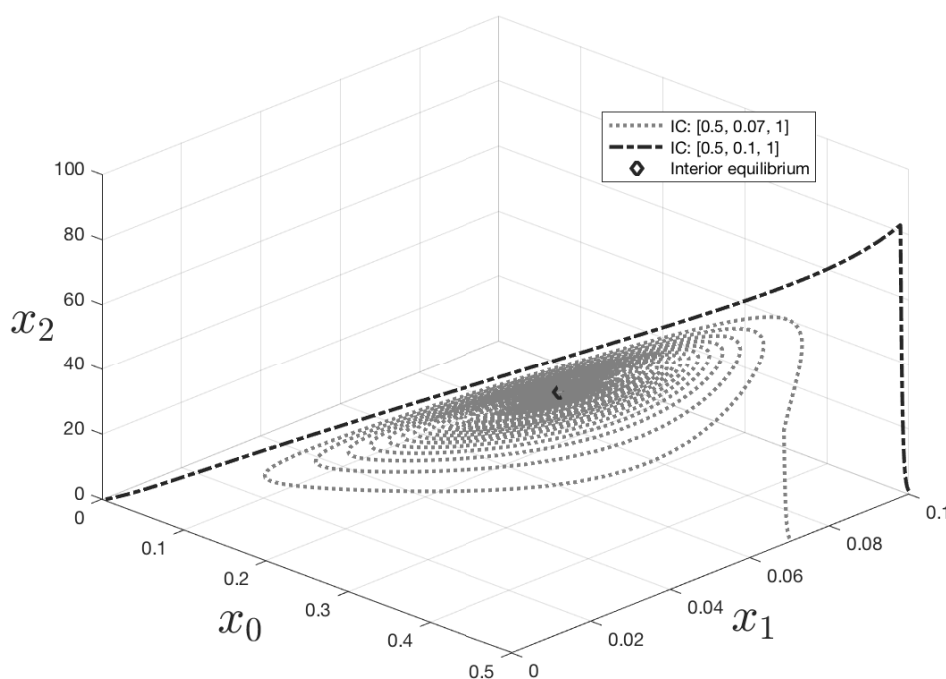


Figure 3. Phase space of system (3.7) with $\alpha = 0.01$, $u_f = 0.5$, $u_g = 0.0006$, and $u_h = 0.3$.

We can see that the Hopf bifurcation occurs between $u_h = 0.05$ and $u_h = 0.3$. The stable periodic orbit is no longer present, and the interior equilibrium is stable. Once again, the boundary equilibrium ${}_{(100)}\mathcal{E}$ is stable, and thus we observe bistability in the system.

It is worth noticing that increasing u_h had a stabilising effect on the system (actually, this type of behaviour applies also to u_f and u_g). This result is especially important in the context of the phenomenon modelled, since the most desirable situation happens when the production of methane is not fluctuating. Variable rates of gas production can result in decreased productivity of the biogas plant.

4.3. Persistence

The notion of persistence is particularly important in modelling biological phenomena. Roughly speaking, we say that a system is persistent if all the species with positive initial populations survive. The formal definition is as follows.

Definition 4.1. The system

$$\begin{aligned}x'_i &= x_i f_i(x_1, x_2, \dots, x_n), \\x_i(0) &= x_{i0} \geq 0, \quad i = 1, 2, \dots, n,\end{aligned}$$

is said to be weakly persistent if

$$\limsup_{t \rightarrow \infty} x_i(t) > 0, \quad i = 1, 2, \dots, n$$

for every trajectory with positive initial conditions, and is said to be persistent if

$$\liminf_{t \rightarrow \infty} x_i(t) > 0, \quad i = 1, 2, \dots, n$$

for every trajectory with positive initial conditions. This system is said to be uniformly persistent if there exists a positive number ϵ such that

$$\liminf_{t \rightarrow \infty} x_i(t) \geq \epsilon, \quad i = 1, 2, \dots, n$$

for every trajectory with positive initial conditions.

To prove that system (3.7) is persistent, we will use the Butler-McGehee Lemma [16] repeatedly.

Lemma 4.2. Assume that x^* is a hyperbolic equilibrium point of the system

$$\begin{aligned}x' &= f(x), \\x(0) &= x_0,\end{aligned}$$

with $x \in \mathbb{R}^n$ and $f : \mathbb{R}^n \rightarrow \mathbb{R}^n$, where f is continuously differentiable. Assume also that x^* is in $\omega(x_0)$, the omega limit set of $\gamma^+(x_0)$ (the positive semi-orbit through x_0), but is not the entire omega limit set. Then $\omega(x_0)$ has nontrivial (i.e., different from x^*) intersection with the stable and unstable manifolds of x^* .

As we already noticed in Section 4.2, there are values of the parameters where one of the boundary equilibria and the interior equilibrium are both asymptotically stable, and hence system (3.7) is not persistent, even though an interior equilibrium point exists. We will thus focus on the cases for which no boundary equilibrium point of system (3.7) is stable.

Theorem 4.2. Let system (3.7) have the following equilibria configuration (as represented schematically in Figure 4):

Equilibrium	Number of eigenvalues with positive real part	Number of eigenvalues with negative real part
${}_{(000)}\mathcal{E}$	2	1
${}_{(100)}\mathcal{E}$	1	2
${}_{(001)}\mathcal{E}$	1	2
${}_{(110)}\mathcal{E}$	1	2

Then system (3.7) is persistent.

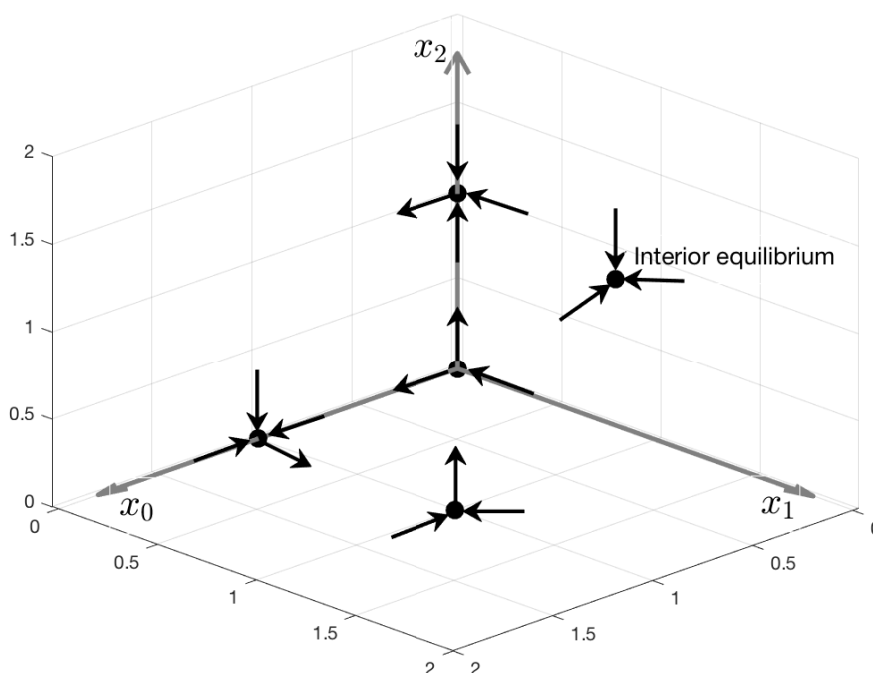


Figure 4. Schematic representation of the equilibria configuration occurring in the hypothesis of Theorem 4.2. Black arrows represent stable and unstable manifolds of each of the equilibrium (marked by the dots). In the example for the parameters we select in model (3.7) to illustrate this theorem (see Eq (4.6)), there is an asymptotically stable interior equilibrium (as shown). However, this is not necessary for the proof of Theorem 4.2.

Proof. Since planes x_0x_1 , x_0x_2 , and x_1x_2 are invariant, we know where the stable and unstable manifolds of the boundary equilibria lie. This is represented in a schematic way in Figure 4. Keeping this picture in mind should make the following argument much more transparent. Assume that a solution $\vec{x}(t) = (x_0(t), x_1(t), x_2(t))$ with initial condition $\vec{x}^{(0)} = (x_0^{(0)}, x_1^{(0)}, x_2^{(0)})$, where $x_i^{(0)} > 0$, $i = 0, 1, 2$, is given. We show that no point of the omega limit set has a zero coordinate using proof by contradiction.

First, assume that $_{(000)}\mathcal{E}$ belongs to $\omega(\gamma^+(\vec{x}^{(0)}))$, the omega limit set of $\gamma^+(\vec{x}^{(0)})$. Since $_{(000)}\mathcal{E}$ is a saddle point with one-dimensional stable manifold restricted to the x_1 -axis, it is not the entire omega limit set $\omega(\gamma^+(\vec{x}^{(0)}))$. Hence, by Lemma 4.2, there is a point $x^* \neq _{(000)}\mathcal{E}$ in both $\omega(\gamma^+(\vec{x}^{(0)}))$ and $W^s(_{(000)}\mathcal{E})$, the stable manifold of $_{(000)}\mathcal{E}$. The entire orbit through any point in an omega limit set is also in the omega limit set. The stable manifold of $_{(000)}\mathcal{E}$ is the x_1 -axis, and the x_1 -axis is unbounded. By Lemma 3.1, all orbits of system (3.7) are bounded, and hence the omega limit set of any orbit of system (3.7) is bounded. This contradicts the existence of such an x^* . Thus $_{(000)}\mathcal{E} \notin \omega(\gamma^+(\vec{x}^{(0)}))$.

Next, assume that $_{(001)}\mathcal{E} \in \omega(\gamma^+(\vec{x}^{(0)}))$. Since $_{(001)}\mathcal{E}$ is a saddle point with two-dimensional stable manifold restricted to the x_0x_1 -plane, $\{_{(001)}\mathcal{E}\}$ is not the entire omega limit set $\omega(\gamma^+(\vec{x}^{(0)}))$. Thus, by Lemma 4.2, there is a point $x^* \in \omega(\gamma^+(\vec{x}^{(0)})) \cap W^s(_{(001)}\mathcal{E}) \setminus \{_{(001)}\mathcal{E}\}$. Since the stable manifold

$W^s({}_{(001)}\mathcal{E})$ lies entirely in the x_1x_2 -plane, and the entire orbit through x^* is in $\omega(\gamma^+(\vec{x}^{(0)}))$, by the analysis in Subsection 4.1, this orbit becomes unbounded in backward time. This contradiction shows that ${}_{(001)}\mathcal{E} \notin \omega(\gamma^+(\vec{x}^{(0)}))$.

Now, assume that ${}_{(100)}\mathcal{E} \in \omega(\gamma^+(\vec{x}^{(0)}))$. Similarly as in the previous cases, this implies that there exists a point $x^* \in \omega(\gamma^+(\vec{x}^{(0)})) \cap W^s({}_{(100)}\mathcal{E}) \setminus \{{}_{(100)}\mathcal{E}\}$. This time the stable manifold $W^s({}_{(100)}\mathcal{E})$ is two-dimensional and lies entirely in the x_0x_2 -plane. By the analysis in Subsection 4.1, the entire orbit through x^* (which belongs to $\omega(\gamma^+(\vec{x}^{(0)}))$) becomes unbounded in backward time or its closure contains ${}_{(001)}\mathcal{E}$. This contradiction proves that ${}_{(100)}\mathcal{E} \notin \omega(\gamma^+(\vec{x}^{(0)}))$.

Now, assume that ${}_{(110)}\mathcal{E} \in \omega(\gamma^+(\vec{x}^{(0)}))$. Again, $\{{}_{(110)}\mathcal{E}\}$ is not the entire omega limit set $\omega(\gamma^+(\vec{x}^{(0)}))$, so there exists a point $x^* \in \omega(\gamma^+(\vec{x}^{(0)})) \cap W^s({}_{(110)}\mathcal{E}) \setminus \{{}_{(110)}\mathcal{E}\}$. This point lies in the x_0x_1 -plane, since $W^s({}_{(110)}\mathcal{E})$ is two-dimensional and is entirely contained in this plane. As in the previous cases, the entire orbit through x^* is in $\omega(\gamma^+(\vec{x}^{(0)}))$. Since there are no periodic orbits in the x_0x_1 face, and since $\{{}_{(100)}\mathcal{E}\} \notin \omega(\gamma^+(\vec{x}^{(0)}))$, the orbit becomes unbounded in backward time. This contradiction proves that ${}_{(110)}\mathcal{E} \notin \omega(\gamma^+(\vec{x}^{(0)}))$.

Finally, consider any $\widehat{x} = (\widehat{x}_0, \widehat{x}_1, \widehat{x}_2)$, such that $\widehat{x}_i = 0$ for at least one $i = 0, 1, 2$, and assume that $\widehat{x} \in \omega(\gamma^+(\vec{x}^{(0)}))$. Then, the entire orbit through \widehat{x} is in $\omega(\gamma^+(\vec{x}^{(0)}))$. But since this orbit lies entirely in either x_0x_1 , x_1x_2 , or x_0x_2 face, it converges to one of the boundary equilibria. This implies that this boundary equilibrium is in $\omega(\gamma^+(\vec{x}^{(0)}))$, and this possibility has been eliminated in the previous part of the proof.

We have therefore proven that

$$\liminf_{t \rightarrow \infty} x_i(t) > 0, \quad i = 0, 1, 2,$$

i.e., that system (3.7) is persistent. □

An example satisfying the assumptions of Theorem 4.2 occurs for

$$\alpha = 0.0002, \quad u_f = 0.6, \quad u_g = 0, \quad u_h = 0.1. \quad (4.6)$$

Persistence can also be observed with the addition of phenol, i.e., with $u_g > 0$.

Theorem 4.3. *Let system (3.7) have the following equilibria configuration (as represented schematically in Figure 5):*

Equilibrium	Number of eigenvalues with positive real part	Number of eigenvalues with negative real part
${}_{(000)}\mathcal{E}$	2	1
${}_{(100)}\mathcal{E}$	1	2
${}_{(001)}\mathcal{E}$	1	2
${}_{(011)}\mathcal{E}$	1	2
${}_{(110)}\mathcal{E}$	1	2

Then system (3.7) is persistent.

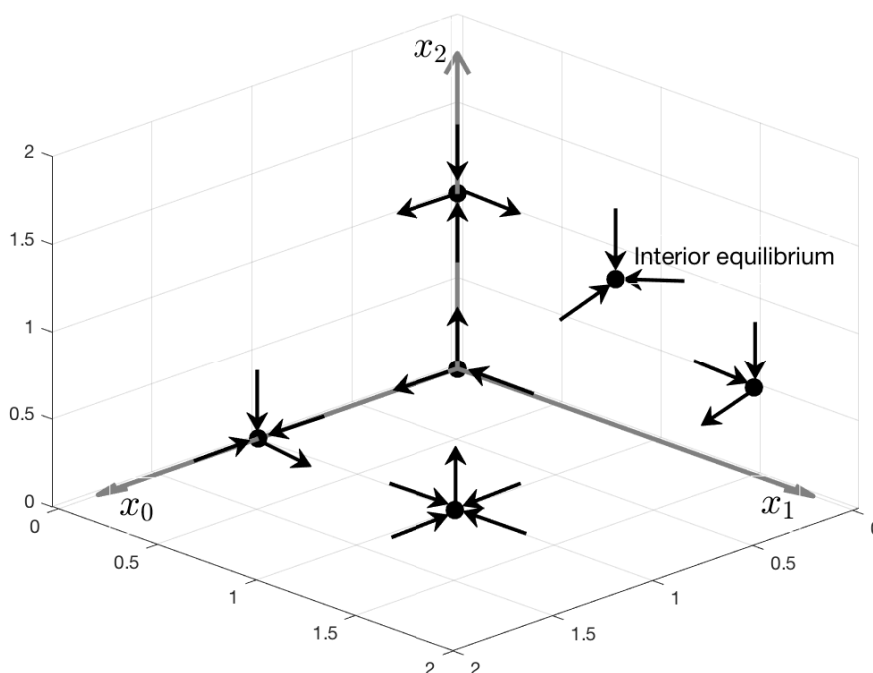


Figure 5. Schematic representation in phase space of the equilibria configuration occurring in the hypothesis of Theorem 4.3. Black arrows represent stable and unstable manifolds of each of the equilibrium (marked by the dots). In the example for the parameters we select in model (3.7) to illustrate this theorem (see Eq (4.7)), there is an asymptotically stable interior equilibrium (as shown). However, this is not necessary for the proof of Theorem 4.3.

Proof. The idea behind this proof is very similar to the method presented in the proof of Theorem 4.2. Let $\vec{x}(t) = (x_0(t), x_1(t), x_2(t))$ be a solution of system (3.7) with initial condition $\vec{x}^{(0)} = (x_0^{(0)}, x_1^{(0)}, x_2^{(0)})$, where $x_i^{(0)} > 0$, $i = 0, 1, 2$. Since the stable and unstable manifolds of all of the equilibria, except ${}_{(001)}\mathcal{E}$ and ${}_{(011)}\mathcal{E}$, have the same configuration as in the hypothesis of Theorem 4.2, the argument eliminating them from the omega limit set of $\gamma^+(\vec{x}^{(0)})$ is exactly the same and we only need to focus on ${}_{(001)}\mathcal{E}$ and ${}_{(011)}\mathcal{E}$.

Assume that ${}_{(001)}\mathcal{E} \in \omega(\gamma^+(\vec{x}^{(0)}))$. Since ${}_{(001)}\mathcal{E}$ is a saddle point with one-dimensional stable manifold restricted to the x_2 -axis, we have $\omega(\gamma^+(\vec{x}^{(0)})) \setminus \{{}_{(001)}\mathcal{E}\} \neq \emptyset$. Hence, by Lemma 4.2, there is a point $x^* \in \omega(\gamma^+(\vec{x}^{(0)})) \cap W^s({}_{(001)}\mathcal{E}) \setminus \{{}_{(001)}\mathcal{E}\}$. The entire orbit through x^* also belongs to $\omega(\gamma^+(\vec{x}^{(0)}))$ and either becomes unbounded in backward time or converges to ${}_{(000)}\mathcal{E}$. Since all orbits of system (3.7) are bounded and ${}_{(000)}\mathcal{E} \notin \omega(\gamma^+(\vec{x}^{(0)}))$, we obtain a contradiction. Hence, ${}_{(001)}\mathcal{E} \notin \omega(\gamma^+(\vec{x}^{(0)}))$.

Next, assume that ${}_{(011)}\mathcal{E} \in \omega(\gamma^+(\vec{x}^{(0)}))$. Since ${}_{(011)}\mathcal{E}$ is a saddle point with two-dimensional stable manifold restricted to the x_1x_2 -plane (it is repelling into the interior), we have $\omega(\gamma^+(\vec{x}^{(0)})) \setminus \{{}_{(011)}\mathcal{E}\} \neq \emptyset$. By Lemma 4.2, there exists a point $x^* \in \omega(\gamma^+(\vec{x}^{(0)})) \cap W^s({}_{(011)}\mathcal{E}) \setminus \{{}_{(011)}\mathcal{E}\}$. The entire orbit through x^*

belongs to $\omega(\gamma^+(\vec{x}^{(0)}))$ and either becomes unbounded in backward time or converges to ${}_{(000)}\mathcal{E}$ or ${}_{(001)}\mathcal{E}$. We have previously shown in Subsection 4.1 that there are no periodic orbits in the x_1x_2 face. Since we have already proven that ${}_{(000)}\mathcal{E} \notin \omega(\gamma^+(\vec{x}^{(0)}))$ and ${}_{(001)}\mathcal{E} \notin \omega(\gamma^+(\vec{x}^{(0)}))$, we obtain a contradiction. This proves that ${}_{(011)}\mathcal{E} \notin \omega(\gamma^+(\vec{x}^{(0)}))$.

Finally, consider any $\widehat{x} = (\widehat{x}_0, \widehat{x}_1, \widehat{x}_2)$, such that $\widehat{x}_i = 0$ for at least one $i = 0, 1, 2$, and assume that $\widehat{x} \in \omega(\gamma^+(\vec{x}^{(0)}))$. Then, the entire orbit through \widehat{x} is in $\omega(\gamma^+(\vec{x}^{(0)}))$. But since this orbit lies entirely in either the x_0x_1 , x_1x_2 , or x_0x_2 face, it converges to one of the boundary equilibria. This implies that this boundary equilibrium is in $\omega(\gamma^+(\vec{x}^{(0)}))$. But this possibility has been eliminated in the previous part of the proof. \square

An example satisfying the assumptions of Theorem 4.3 occurs for

$$\alpha = 0.0002, \quad u_f = 0.6, \quad u_g = 0.00015, \quad u_h = 0.1. \quad (4.7)$$

Remark 1. Interestingly enough, in many cases of models describing biological phenomena, persistence already implies uniform persistence. The rigorous results were obtained in [17]. In our context, the key theorem from [17] states that if \mathcal{F} is a dynamical system for which \mathbb{R}_+^n and $\partial\mathbb{R}_+^n$ are invariant, then \mathcal{F} is uniformly persistent provided that

1. \mathcal{F} is dissipative (meaning that $\forall x \in \mathbb{R}_+^n \ \omega(x) \neq \emptyset$ and $\bigcup_{x \in \mathbb{R}_+^n} \omega(x)$ has compact closure),
2. \mathcal{F} is weakly persistent,
3. $\partial\mathcal{F}$ (the restriction of \mathcal{F} to the boundary $\partial\mathbb{R}_+^n$) is “isolated”,
4. $\partial\mathcal{F}$ is “acyclic”.

These results can be easily modified [18] so that we consider the flow \mathcal{F} on Ω and $\partial\Omega$, which are positively invariant. The following theorem is proven using results of [17, 18], by checking conditions 1–4 on Ω and $\partial\Omega$.

Theorem 4.4. *Under the hypotheses of Theorem 4.2 or Theorem 4.3, system (3.7) is uniformly persistent.*

Proof. In our case, the positively invariant set Ω , on which we analyse system (3.7) is bounded. Hence, condition 1 is satisfied. Condition 2 holds by Theorem 4.2 (persistence implies weak persistence). In our context condition 3 is satisfied, because the omega limit set on $\partial\Omega$ consists of a finite number of hyperbolic equilibria. Condition 4 is satisfied because the boundary equilibria are not cyclically linked, i.e., there is no cyclic chain of heteroclinic orbits joining them. Thus, we have shown not only persistence, but also uniform persistence of system (3.7) in the cases when the hypotheses of Theorem 4.2 or Theorem 4.3 are satisfied. \square

We finish this subsection by extending the uniform persistence to the original six dimensional system (2.1).

Theorem 4.5. *Under the hypotheses of Theorem 4.2 or Theorem 4.3, the six dimensional system (2.1) is uniformly persistent.*

Proof. Notice that if $\vec{X}_0 = (x_0(0), x_1(0), x_2(0), s_0(0), s_1(0), s_2(0))$ with $x_i(0) > 0$, $s_i(0) > 0$, $i = 0, 1, 2$, then we necessarily must have $\omega(\vec{X}_0) \in \Omega$. Otherwise, there would exist a point $\vec{p} \in \mathbb{R}_+^6 \setminus \Omega$ and a sequence of times (t_n) with $t_n \rightarrow \infty$ for which the corresponding solution converges to \vec{p} . This would mean that Ω is not globally attracting, which was proven in Lemma 3.2. Moreover, there is only a finite number of equilibria on $\partial\Omega$, with all of their stable manifolds lying entirely in $\partial\Omega$. Thus, if the assumptions of either Theorem 4.2 or Theorem 4.3 hold, by Theorem 4.4 and its proof, the corresponding three-dimensional system is uniformly persistent and the boundary $\partial\Omega$ is acyclic. Hence, we can apply the results of Thieme [19] to conclude that the six-dimensional system (3.1) is also uniformly persistent. \square

4.4. Bifurcation diagrams

As previously stated in Section 4.2, we now study effects on the qualitative behaviour of system (3.7) numerically. We consider α as a bifurcation parameter. Throughout this section, we assume that parameters $\omega_0, \omega_1, \omega_2, \phi_1, \phi_2, K_P$, and K_I are fixed at the values given in Table 1.

We now fix the following parameters

$$u_f = 2, \quad u_g = 0, \quad u_h = 0,$$

and plot a one-parameter bifurcation diagram in α , with x_0 on the y-axis. All simulations were performed using [20].

In Figure 6, we can see that as α decreases, there is a saddle-node bifurcation, resulting in two equilibria ${}_{(110)}\mathcal{E}^{(1)}$ and ${}_{(110)}\mathcal{E}^{(2)}$ appearing (both unstable). Next, there is a transcritical bifurcation with the ${}_{(110)}\mathcal{E}^{(1)}$ equilibrium. This results in the positive equilibrium moving into the interior of the admissible region, Ω . After that, a saddle-node of limit cycles bifurcation occurs that gives birth to stable and unstable periodic orbits. The ${}_{(111)}\mathcal{E}$ equilibrium (unstable), undergoes a Hopf bifurcation, and as a consequence it becomes asymptotically stable, and the stable periodic orbit disappear. Since these bifurcations occur for a narrow range of α , a close-up is presented in Figure 7. Existence of a stable periodic orbit represents a case in which all three populations oscillate indefinitely, and hence the production of methane fluctuates. As already mentioned in Section 4.2, this situation is not a desirable one, because it might result it decreased productivity by the biogas plant. The unstable periodic orbit acts as a separatrix, giving the border of the basin of attraction of two asymptotically stable equilibria in the case of bistability.

Since by the conservation principles (3.6), $s_0 = u_f - x_0$, the bifurcation diagram in α with s_0 on the y-axis is similar to the one presented in Figure 6. The amount of chlorophenol in the system is inversely proportional to the concentration of the phenol degrader. As the dilution rate α decreases, the concentration of the chlorophenol degrader in the interior equilibrium increases, and as a consequence, the amount of chlorophenol decreases. It thus suggests that operating on lower dilution rates results in the most desirable dynamics, i.e., an asymptotically stable interior equilibrium and fast chlorophenol removal.

To extend the previous analysis, we now fix the following parameters:

$$u_g = 0, \quad u_h = 0.1,$$

and plot a two-parameter bifurcation diagram of system (3.7), choosing α and u_f as the bifurcation parameters. Each region of the diagram is labeled and the corresponding dynamics are represented schematically in the surrounding figures in phase space. Black dashed curves correspond to saddle-node of equilibria bifurcations (LP), black solid curves represent saddle-node of limit cycles bifurcations (SNLC), black dotted curves depict Hopf bifurcations (HB), and grey solid curves represent transcritical bifurcations (BP). We also depict the predicted heteroclinic bifurcation by a grey dashed curve which lies very close to the BP curve.

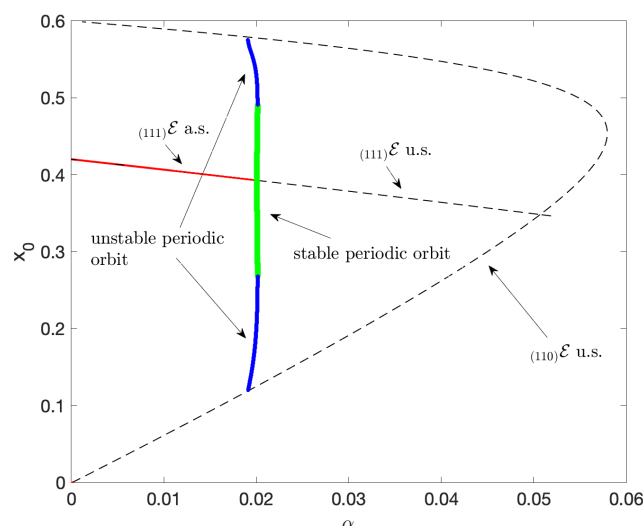


Figure 6. One-parameter bifurcation diagram of system (3.7) with α as the bifurcation parameter and $u_f = 2$, $u_g = 0$, $u_h = 0$.

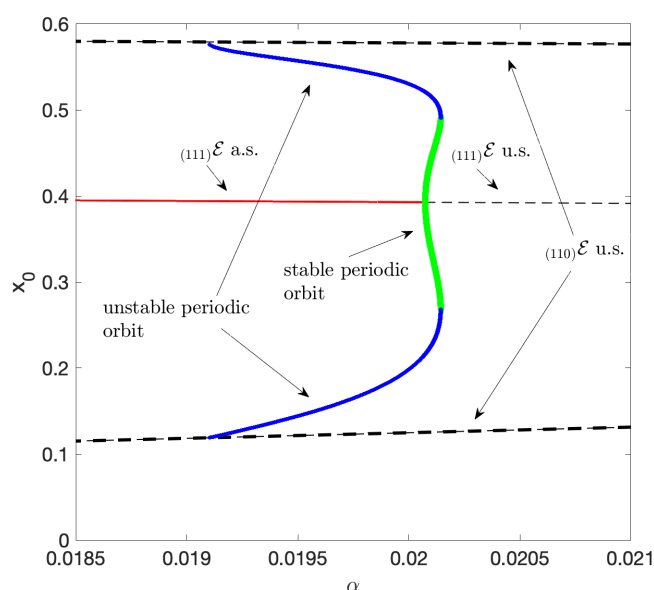


Figure 7. Close-up of the one-parameter bifurcation diagram represented in Figure 6.

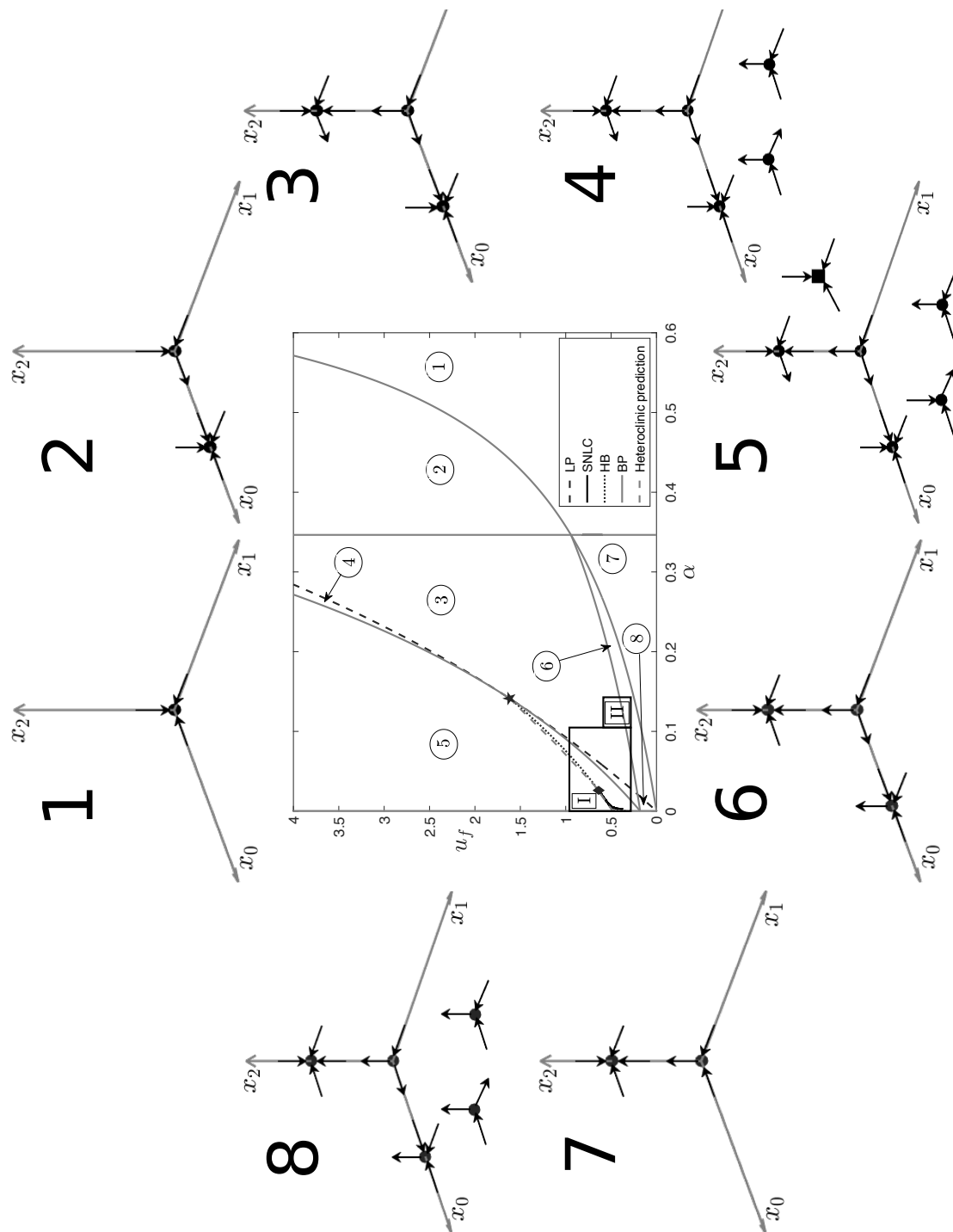


Figure 8. Two-parameter bifurcation diagram with bifurcation parameters α and u_f of system (3.7) with $u_g = 0$ and $u_h = 0.1$ and the corresponding phase space diagrams for each region in parameter space.

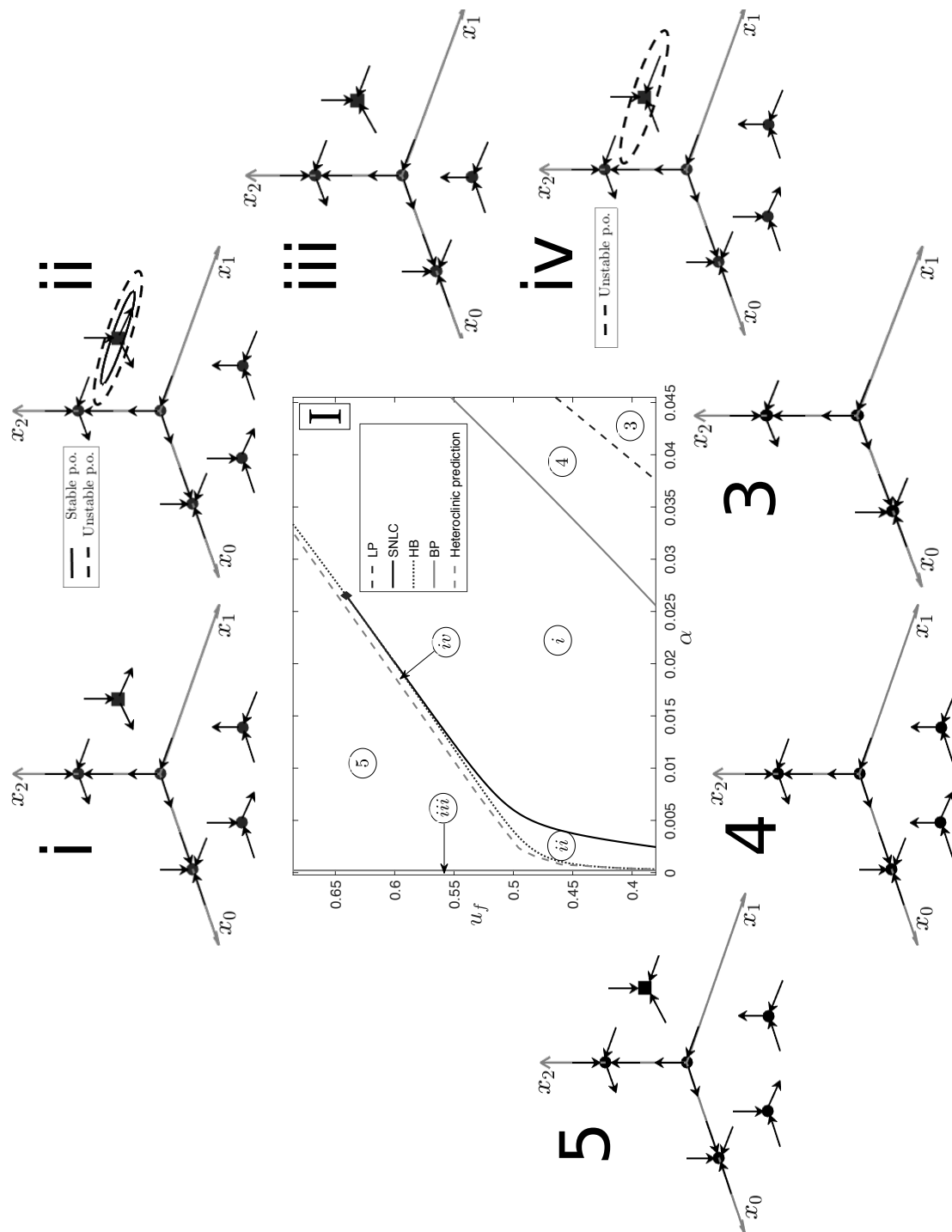


Figure 9. Close-up on region I of Figure 8. The SNLC curve intersects the HB curve at Bautin bifurcation. This results in the change of criticality of the Hopf bifurcation from supercritical (on the left) to subcritical (on the right).

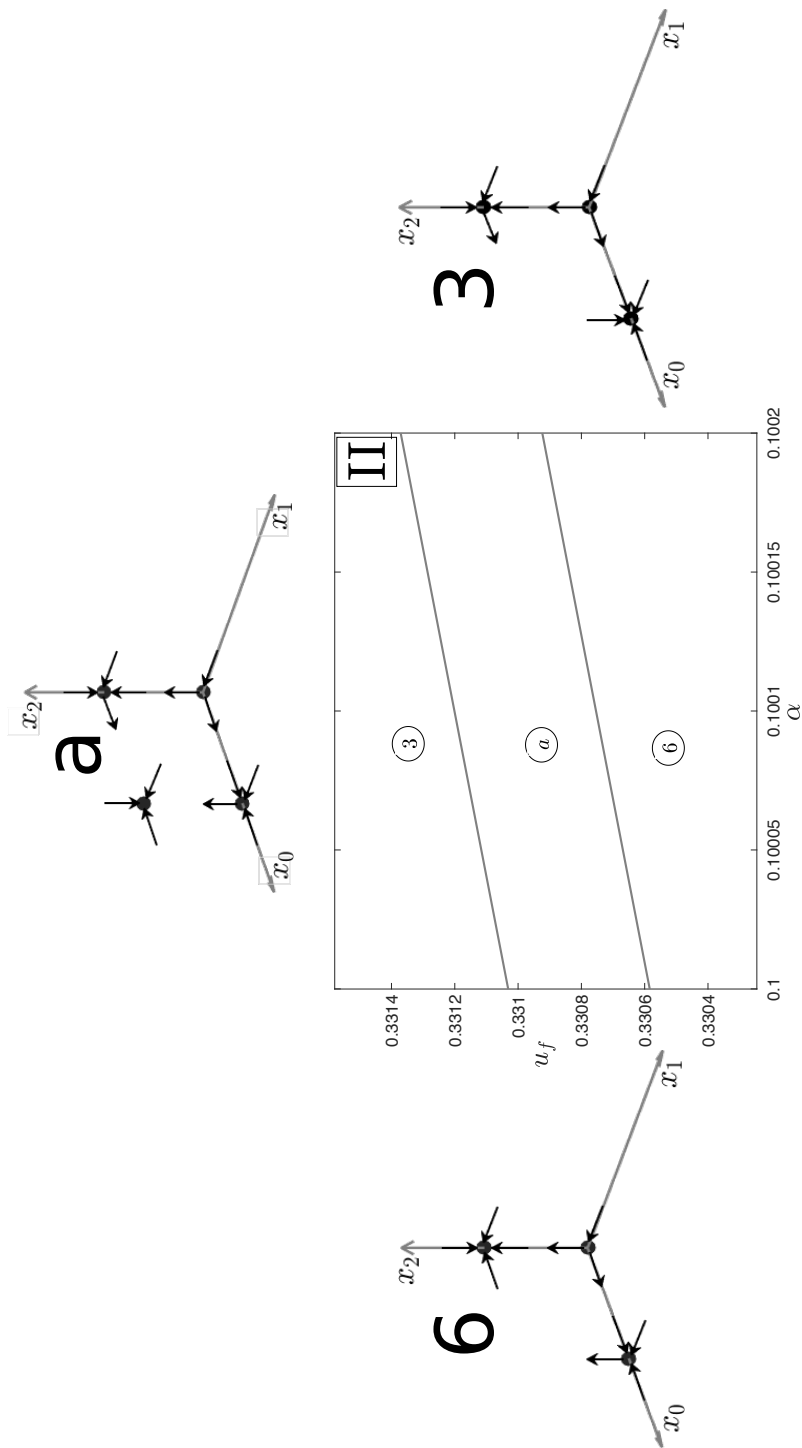


Figure 10. Close-up of region II of Figure 8.

We can see in Figures 8–10, that varying two parameters at the same time can demonstrate much more complicated dynamics than in the case of one-parameter bifurcation diagrams. There is a generalised Hopf bifurcation, at the point at which the Hopf curve intersects the saddle-node of limit cycles curve. This is the point where the criticality of the Hopf bifurcation changes from supercritical to subcritical, moving from left to right. The unstable periodic orbit disappears through a heteroclinic bifurcation. There are two heteroclinic orbits that form a cycle that joins the two equilibria in the x_0x_1 face, then passes into the interior, and then goes back to the boundary in the x_0x_1 face. The point at which the Hopf, homoclinic, and saddle-node of limits cycles curves intersect, represents the Bogdanov-Takens bifurcation.

From the biological viewpoint, the most interesting dynamics occurs in regions 5 and *iii*. There, the interior equilibrium is asymptotically stable. In the case of region 5 we also observe bistability with the $_{(100)}\mathcal{E}$ equilibrium. In region *iii*, there is uniform persistence, and thus an interior compact attractor is present. As was previously anticipated by the analysis of the one-parameter bifurcation diagram, operating at low dilution rates is the most desirable approach. If α is small enough, it is possible to remain in region *iii*, even for high inflow rate u_f .

5. Conclusions

In this work we have generalised the approach presented in [9] by including multiple substrate inflow in the chemostat, while maintaining generality (in most cases) with respect to the exact form of the growth functions. We observed that allowing the inflow of multiple substrates resulted in much more complex dynamics of the system. For example, eight steady states are possible. We also observed that external addition of substrates (phenol and hydrogen) can result in bistability—two equilibria can simultaneously be asymptotically stable. As well, there can be an orbitally asymptotically stable periodic orbit with all of the populations surviving and an asymptotically stable equilibrium with only the chlorophenol degrader population surviving.

We have also confirmed the findings of the previous analysis in [9], where numerical evidence of the occurrence of a supercritical Hopf bifurcation was given. Theoretical conditions for the existence of a Hopf bifurcation were provided in the case of specific forms of the growth functions. Varying any one of the three parameters: chlorophenol, phenol, and hydrogen inflow rates, was shown to result in a Hopf bifurcation. Theoretical results for varying the dilution rate as the bifurcation parameter has been left for future work. However, we have observed numerically, that varying this parameter can result in a Hopf bifurcation and a saddle-node of limit cycles bifurcation. Our numerical investigations also showed that increasing the inflow rate of the substrates has a stabilising effect on the entire system. From a biological engineering point of view, in a bioreactor treating a monochlorophenol rich waste stream, instability would typically be undesirable in terms of process performance. Therefore, identification of control strategies to avoid periodic behaviour is an important aspect of this work.

Another result, particularly important for engineering applications, concerns the persistence of the system for a range of parameter sets. Knowing when the microbial populations survive is again crucial from a process control perspective, and it is one of the main theoretical results of this work. We have proven that in two configurations of equilibria (in both cases all the boundary equilibria are saddle points) we observe not only persistence, but also uniform persistence, a much stronger result. These

situations occur when there is an inflow of all three substrates, but also when phenol addition is not considered (i.e., when $u_g = 0$).

Although we now know much more about the dynamics of the system, it is not fully understood. This follows from the numerical results provided by the two-parameter bifurcation diagrams. The analyses reveals that varying the dilution rate and the chlorophenol inflow simultaneously, can lead to a Bogdanov-Takens and a Bautin (generalised Hopf) bifurcations. Also, for the cases of bistability, where both a boundary and the interior equilibrium are asymptotically stable, it is of great importance to empiricists to have an estimation of the basins of attraction of these equilibria. This result is usually difficult to obtain theoretically, however numerical estimations are possible. Another factor that is of interest would be the inclusion of stochasticity in the model. In practice, even if the interior equilibrium is globally asymptotically stable, one of the microorganisms may become extinct. This might occur when a population is very small, and the stochastic noise effects result in the solution curve reaching one of the invariant faces of the admissible region.

Anecdotal, there has been some resistance to using reduced order models, of the type described here. Some researchers consider them too removed from the systems they represent to be of practical use. Without experimental results to compare against model predictions, they remain mostly theoretical constructs limited by the underlying assumptions and simplifications imposed. However, we can look to emerging disciplines such as synthetic biology to help bridge the theoretical and the applied [21]. Recent studies have shown that synthetically derived anaerobic communities are able to confirm model predictions and provide insight into the ecology and dynamics of microbial communities that are relevant in practice [22]. For example, we have shown that, in a region of unstable dynamics for a given set of operational parameters and initial conditions, addition of extraneous hydrogen results in an asymptotically stable equilibrium by ensuring survival of the two hydrogen consumers. Hydrogen is a key substrate in methanogenic systems, but process stabilisation by its addition has only recently been suggested [6, 7]. We believe this work provides a basis from which experimental studies describing microbial food-webs with complex, high-order interactions can be conducted with *a posteriori* knowledge of the anticipated behaviour.

Acknowledgments

Matthew J. Wade acknowledges the support from the European Union's Horizon 2020 research and innovation programme under the Marie Skłodowska-Curie Grant Agreement No. 702408 (DRAMATIC). Gail S.K. Wolkowicz acknowledges support from the Natural Sciences and Engineering Council of Canada (NSERC) Discovery Grant with accelerator supplement.

Conflict of interest

The Authors declare no conflict of interest in this work.

References

1. M. J. Wade, R. W. Pattinson, N. G. Parker, J. Doling, Emergent behaviour in a chlorophenol-mineralising three-tiered microbial 'food web', *J. Theor. Biol.*, **389** (2016), 171–186.

2. C. Mazur, W. Jones, C. Tebes-Stevens, H_2 consumption during the microbial reductive dehalogenation of chlorinated phenols and tetrachloroethene, *Biodegradation*, **14** (2003), 285–295.
3. L. Levén, K. Nyberg, A. Schnürer, Conversion of phenols during anaerobic digestion of organic solid waste - a review of important microorganisms and impact of temperature, *J. Env. Manage.*, **95** (2012), 99–103.
4. T. Großkopf, O. Soyer, Microbial diversity arising from thermodynamic constraints, *ISME J.*, **10** (2016), 2725–2733.
5. B. Schink, Energetics of syntrophic cooperation in methanogenic degradation, *Microbiol. Mol. Biol. Rev.*, **61** (1997), 262–280.
6. I. Bassani, P. G. Kougias, L. Treu, I. Angelidaki, Biogas upgrading via hydrogenotrophic methanogenesis in two-stage continuous stirred tank reactors at mesophilic and thermophilic conditions, *Environ. Sci. Technol.*, **49** (2015), 12585–12593.
7. J. Chen, M. J. Wade, J. Dolfig, O. S. Soyer, Increasing sulfate levels show a differential impact on synthetic communities comprising different methanogens and a sulfate reducer, *J. Royal Soc. Interface*, **16** (2019), 20190129.
8. N. W. Smith, P. R. Shorten, E. H. Altermann, N. C. Roy, W. C. McNabb, Hydrogen cross-feeders of the human gastrointestinal tract, *Gut Microbes*, **10** (2019), 270–288.
9. T. Sari, M. J. Wade, Generalised approach to modelling a three-tiered microbial food-web, *Math. Biosci.*, **291** (2017), 21–37.
10. M. El Hajji, N. Chorfi, M. Jleli, Mathematical modelling and analysis for a three-tiered microbial food web in a chemostat, *Electron. J. Differ. Eq.*, **255** (2017), 1–13.
11. S. Nouaoura, N. Abdellatif, R. Fekih-Salem, T. Sari, Mathematical analysis of a three-tiered model of anaerobic digestion, Preprint, hal-02540350v2.
12. S. Nouaoura, R. Fekih-Salem, N. Abdellatif, T. Sari, Mathematical analysis of a three-tiered food-web in the chemostat, Preprint, hal-02878246.
13. Y. Kuznestov, *Elements of Applied Bifurcation Theory*, Springer-Verlag, New York, 2004.
14. Maple [Software]. Version 18.02. Waterloo Maple Inc., Waterloo, Ontario, 2018. Available from: <https://maplesoft.com>.
15. MATLAB [Software]. Version 9.5.0.944444 (R2018b). The MathWorks Inc., Natick, Massachusetts, 2018. Available from: <https://www.mathworks.com>.
16. H. L. Smith, P. Waltman, *The Theory of the Chemostat: Dynamics of Microbial Competition (Cambridge Studies in Mathematical Biology)*, Cambridge University Press, 1995.
17. G. J. Butler, H. I. Freedman, P. Waltman, Uniformly persistent systems, *P. Am. Math. Soc.*, **96** (1986), 425–430.
18. G. J. Butler, G. S. K. Wolkowicz, Predator-mediated competition in the chemostat, *J. Math. Biol.*, **24** (1986), 167–191.
19. H. R. Thieme, Convergence results and a Poincare-Bendixson trichotomy for asymptotically autonomous differential equations, *J. Math. Biol.*, **30** (1992), 755–763.

20. XPPAUT [Software]. Version 8.0. Dr. Bard Ermentrout, Dept of Mathematics, University of Pittsburgh, Pittsburgh PA, 2016. Available from: <http://www.math.pitt.edu/~bard/xpp/xpp.html>.
21. M. El Karoui, M. Hoyos-Flight, L. Fletcher, Future trends in synthetic biology—a report, *Front. Bioeng. Biotechnol.*, **7** (2019), 175.
22. H. Delattre, J. Chen, M. J. Wade, O. S. Soyer, Thermodynamic modelling of synthetic communities predicts minimum free energy requirements for sulfate reduction and methanogenesis, *J. R. Soc. Interface*, **17** (2020), 20200053.



AIMS Press

© 2020 the Author(s), licensee AIMS Press. This is an open access article distributed under the terms of the Creative Commons Attribution License (<http://creativecommons.org/licenses/by/4.0>)